Electronic Supplementary Information

Discovery of an Olivine-type Lithium Manganese Thiophosphate, $LiMnPS_4$, via Building Block Approach

*Srikanth Balijapelly,[a] Kartik Ghosh,[b] Aleksandr V. Chernatynskiy,[c] Amitava Choudhury[a,] **

[a]Department of Chemistry, Missouri University of Science and Technology, Rolla, MO 65409, USA. E-mail: choudhurya@mst.edu

[b]Department of Physics, Astronomy and Materials Sci, Missouri State University, 901 S. National Ave., Springfield, MO 65897, USA

[c]Department of Physics, Missouri University of Science and Technology, Rolla, MO 65409, USA

SI NO	Content	Page No
1	Experimental Section (Synthesis, X-ray crystallography, UV-DRS measurements, Magnetic measurements, Theoretical calculations)	S-3-S-6
Table S1	Atomic coordinates and isotopic thermal displacement parameters	S - 7
Table S2	Selected bond lengths	S - 8
Table S3	Anisotropic thermal displacement parameters	S - 9
Figure S1	As-synthesized DMF washed crystals of $LiMnPS_4$	S - 10
Figure S2	PXRD of $LiMnPS_4$	S - 11
Figure S3	PXRD of Li_3PS_4	S - 12
Figure S4	PXRD of air exposed $LiMnPS_4$	S - 13
Figure S5	EDS spectra and elemental mapping	S -14
Figure S6	Diffuse reflectance plot for Li_3PS_4	S - 15
Figure S7	Total density of states and brillouin zone of primitive orthorhombic lattice	S - 16
Figure S8	$\chi_m T$ versus T plot	S - 17
	References	S-18

Experimental Section:

Synthesis

$LiMnPS_4$ has been synthesized from solid-state metathesis route using γ-Li_3PS_4 and $MnCl_2$. First Li_3PS_4 was synthesized from stoichiometric mixture of Li_2S (4.5 mmol) and P_2S_5 (1.5 mmol) ($1.5Li_2S + 0.5P_2S_5 = Li_3PS_4$). Li_2S and P_2S_5 were ground together inside argon-filled glove box (O_2 < 0.1ppm) and loaded into a carbon coated quartz ampule. The flame sealed quartz ampoule was heated to 700 °C at a rate of 30 °C /h, dwelled for 12 h and subsequently cooled to room temperature at a cooling rate of 35 °C /h. White crystalline powder sample was obtained after breaking the ampoule inside argon filled glove box. Phase pure Li_3PS_4 (1 mmol) and $MnCl_2$ (1 mmol) were ground together in 1:1 ratio in an agate mortar and loaded in carbon coated quartz ampoule. The quartz tube was flame sealed and heated to 500 °C for 48 h, the heating and cooling rates were 25 and 30 °C /h, respectively. A schematic of the reaction is shown in scheme 1. Shiny single chunk containing pale yellow color crystals were obtained after breaking the ampoule inside an argon-filled glove box. To remove the salt (LiCl) byproduct ($Li_3PS_4 + MnCl_2 = LiMnPS_4 + 2LiCl$), the as synthesized single chunk was sonicated in *N,N* dimethylformamide (DMF). The crystals were found to be stable in air for several days. Appropriate crystal was chosen for single crystal X-ray diffraction and the as synthesized crystals/hand ground powder was used for further characterization. A digital photograph showing the as-synthesized $LiMnPS_4$ was provided in ESI (Figure S1).

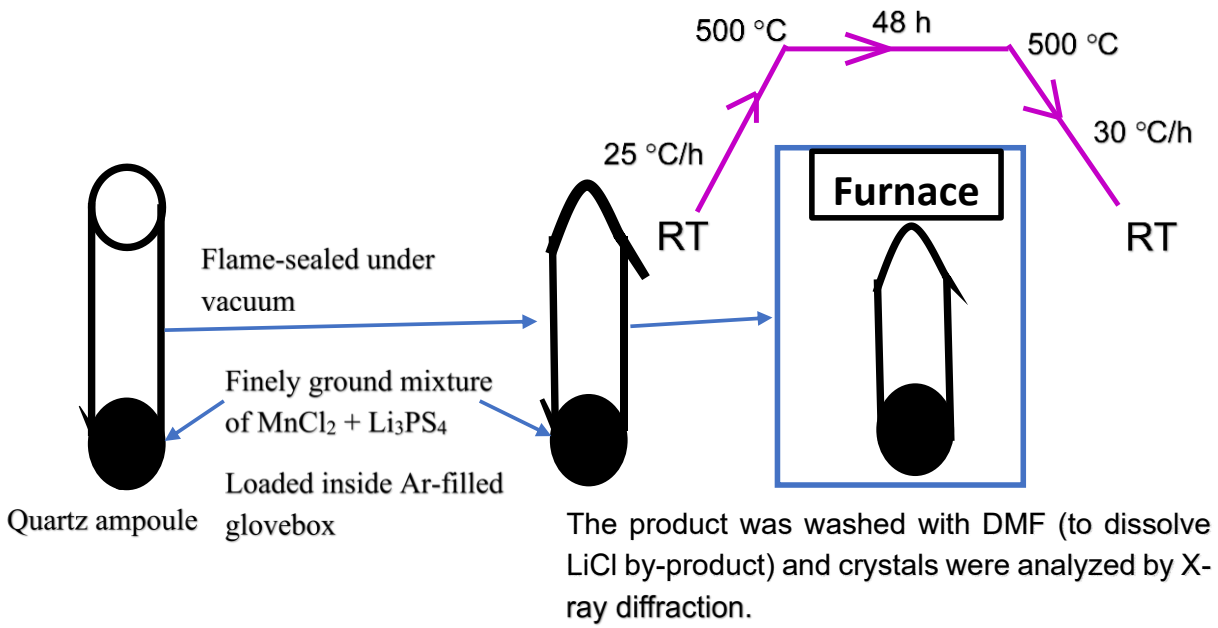

Scheme 1: A schematic showing how the reactions are carried out in sealed ampoules.

X-Ray crystallography

Good quality crystal was chosen for single-crystal X-Ray diffraction on a Bruker smart apex equipped with a sealed tube X-ray source with Mo−Kα radiation (λ = 0.71073 Å). Room temperature diffraction data sets were collected using SMART[1] software with a step of 0.3° in the ω scan and 10 s/ frame exposure time. Program SAINT[2] was used for data integration and SADABS[2] was used for the absorption correction, respectively. SHELXS-97 and difference Fourier syntheses were used to solve the structure.[3] Full-matrix least-square refinement against $|F^2|$ was carried out using the SHELXTL-PLUS suite of programs.[2] The compound crystallizes in orthorhombic crystal system with *Pnma* (No.62) space group. The asymmetric unit consists of three sulfur, one manganese, one phosphorous and one lithium which can be easily located from the difference Fourier map. Absence of unaccounted e-density and reasonably good thermal displacement parameters with low weighted *R* factor wR_2, the charge balanced formula $LiMnPS_4$ was derived based on the 100% occupancies of the atoms. Final refinements including the

refinement of anisotropic thermal parameters were performed using SHELX-2018 embedded in ShelXLe.[4] Selected bond lengths, atomic coordinates along with their isotropic thermal parameters are given in the ESI (Tables S1-S3)

Powder X-Ray diffraction:

Hand ground powder sample in an argon filled glove box was used to collect the laboratory powder X-ray diffraction (PXRD) pattern from a PANalytical X'Pert Pro diffractometer equipped with a Cu Kα anode and a linear array PIXcel detector over a 2θ range of 5−90° with an average scanning rate of 0.0472° s^{-1}. Air-tight cell holder with Kapton film window was used to minimize the air exposure. The PXRD patterns of the as-synthesized and air exposed $LiMnPS_4$ are provided in Figures S2 and S4. The PXRD of the as-synthesized γ–Li_3PS_4 is provided in Figure S3. The PXRD of the $LiMnPS_4$ after air exposure didn't show any change indicating good air and moisture stability.

EDS analysis

Elemental analysis is studied by Scanning electron microscope (SEM) using an TESCAN-ASCAT system equipped with Bruker energy dispersive spectroscopy (EDX). The elemental mapping (Figure S5) shows uniform distribution of Mn, P, and S with ratio's 1.04:1.02:4 which is in very good agreement with the crystallographically-derived composition.

Optical Band Gap Measurements

Optical band gap measurements were performed on a Varian Cary 5000 UV−vis−NIR spectrophotometer equipped with a praying mantis set up. $BaSO_4$ powder (Fisher, 99.2%) was used as an ∼100% reflectance standard, and the Kubelka-Munk[5] function was employed to transform the reflectance into absorption data to find out the band gap. Tauc plot $\alpha h\nu = A(h\nu - E_g)^m$

was employed to estimate the nature of optical band gap, where α is absorption coefficient (Kubelka-Munk function), $h\nu$ is the photon energy, and m = 2 or ½ depending on whether the transition is direct or indirect. $LiMnPS_4$ exhibit linearity in $h\nu$ *vs* $(\alpha h\nu)^{1/2}$ plot, suggesting that the sample possess indirect band gap of 2.36 eV. Diffuse reflectance spectra of γ-Li_3PS_4 shows an indirect band gap of 3.8 eV (Figure S6).

Theoretical calculations

Spin polarized band structure calculations were performed on experimentally determined structure using density functional theory as implemented in Vienna *Ab-intio* Simulations Package (VASP).[6-9] Hybrid functional (HSE06) calculations were employed to describe accurate band structure and estimate the band gap.[10] Kinetic energy cut off was set to 520 eV and Γ centered *k*-point grid size of 2×3×4 was used for Brillouin zone integration. Relaxed atomic structure by the standard DFT with convergence threshold of 10^{-6} eV for total energy and 10^{-3} eV/Å for the maximum force was used for the hybrid functional calculations. All the calculations were performed in ferromagnetic (FM) configuration. The density of states is calculated using gaussian smearing of 0.05 eV.

Magnetic Measurements

The DC magnetic susceptibility was measured at 1 Tesla (1 Tesla = 10000 Oe) magnetic field after zero-field cooling over the temperature range 3.2-300 K in a Quantum Design SQUID magnetometer. Isothermal magnetization at 5 and 300 K was measured in an applied field range of 0 – 5 Tesla. Zero field cooled (ZFC) and field cooled (FC) magnetization data were collected from 3 – 50 K at an applied field of 100 Oe. Variable field magnetization was measured at 5K under ZFC condition in an applied field range of +5 to -5 Tesla. A $\chi_m T$ versus T plot is given Figure S8.

Table S1. Final atomic coordinates and equivalent isotropic displacement parameters for $LiMnPS_4$. U(eq) is defined as 1/3rd of the trace of the orthogonalized U^{ij} tensor.

Atom	Wyckoff	Occupancy	x/a	y/b	z/c	U(Å^2)
Mn(1)	4b	1	0	0	0.5	0.025(1)
P(1)	4c	1	0.0911(1)	0.25	0.1064(2)	0.013(1)
S(1)	8d	1	0.1649(1)	0.0357(1)	0.2428(1)	0.018(1)
S(2)	4c	1	-0.0625(1)	0.25	0.2409(2)	0.016(1)
S(3)	4c	1	0.0947(1)	0.25	-0.2420(1)	0.017(1)
Li(1)	4c	1	-0.2281(7)	0.25	-0.0109(12)	0.030(2)

Table S2. Selected bond lengths for $LiMnPS_4$

Bonds	Distance (Å)	Bonds	Distance (Å)
Mn1 – S2	2.5613(7)	P1 – S3	2.0333(13)
Mn1 – S2$^{\#1}$	2.5613(7)	P1 – S1$^{\#4}$	2.0451(10)
Mn1 – S1$^{\#1}$	2.5696(8)	P1 – S1	2.0451(10)
Mn1 – S1	2.5696(8)	P1 – S2	2.0791(14)
Mn1 – S3$^{\#2}$	2.7087(7)		
Mn1 – S3$^{\#3}$	2.7087(7)		

Symmetry transformations used to generate equivalent atoms:
#1 -x, -y, -z + 1 #2 -x, -y, -z #3 x, y, z+1 #4 x, -y+1/2, z

Table S3. Anisotropic displacement parameters ($Å^2 x 10^3$) for LiMnPS4. The anisotropic displacement factor exponent takes the form: $-2p^2[h^2a^{*2}U^{11} + ... + 2 h k a^* b^* U^{12}]$

Atoms	U^{11}	U^{22}	U^{33}	U^{23}	U^{13}	U^{12}
Mn(1)	30(1)	24(1)	21(1)	8(1)	7(1)	1(1)
P(1)	17(1)	16(1)	7(1)	0	0(1)	0
S(1)	21(1)	21(1)	13(1)	1(1)	1(1)	5(1)
S(2)	15(1)	20(1)	13(1)	0	1(1)	0
S(3)	23(1)	21(1)	7(1)	0	1(1)	0
Li(1)	30(4)	36(4)	25(4)	0	-6(3)	0

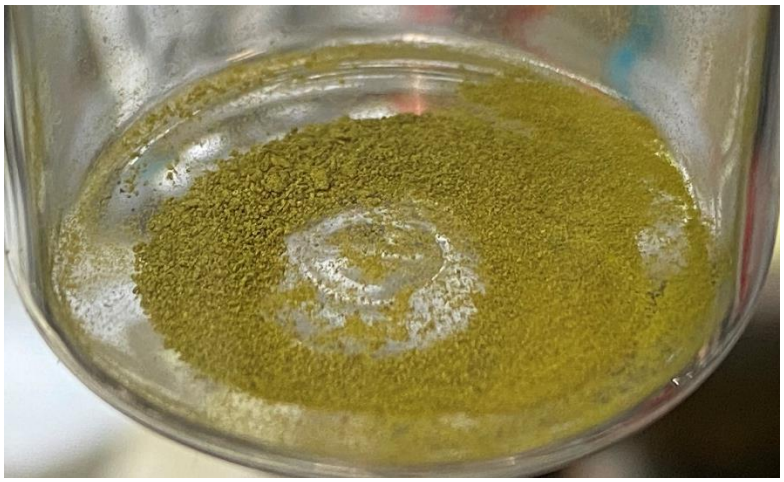

Figure S1: (a) As-synthesized DMF washed crystals of $LiMnPS_4$ synthesized from metathesis route (Li_3PS_4 + $MnCl_2$).

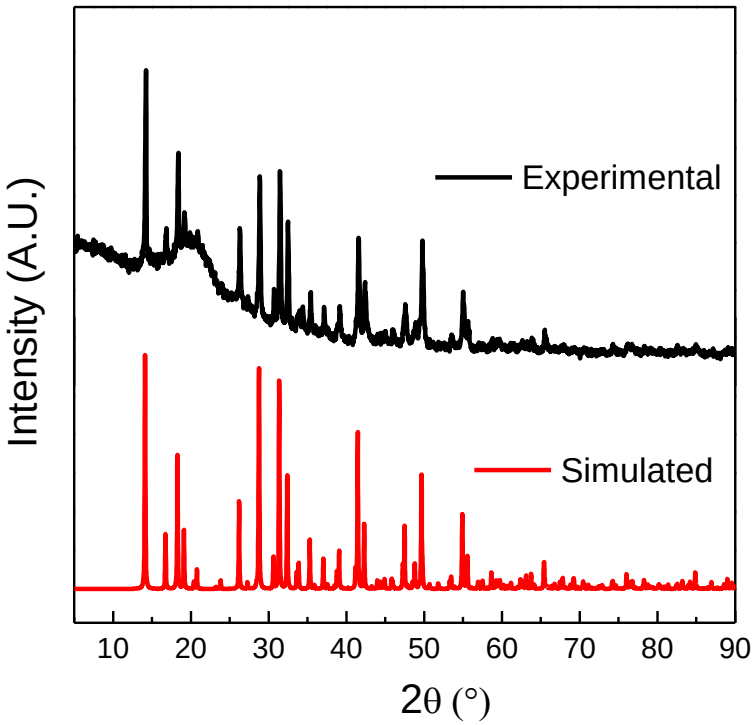

Figure S2: Comparison of simulated and experimental powder X-ray diffraction pattern for $LiMnPS_4$ synthesized from metathesis route (Li_3PS_4 + $MnCl_2$) .

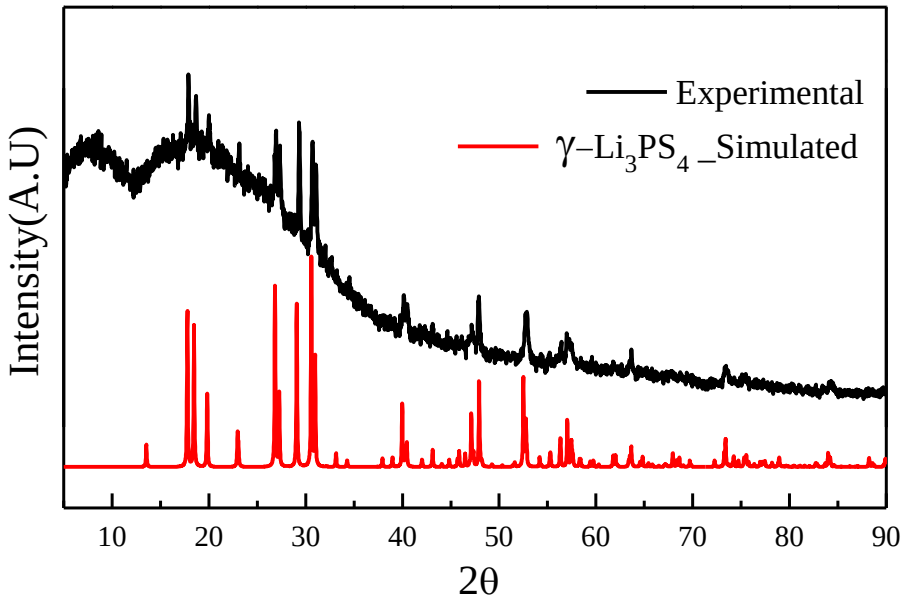

Figure S3: PXRD patterns showing the comparison of experimental Li_3PS_4 with the simulated patterns of γ – Li_3PS_4.

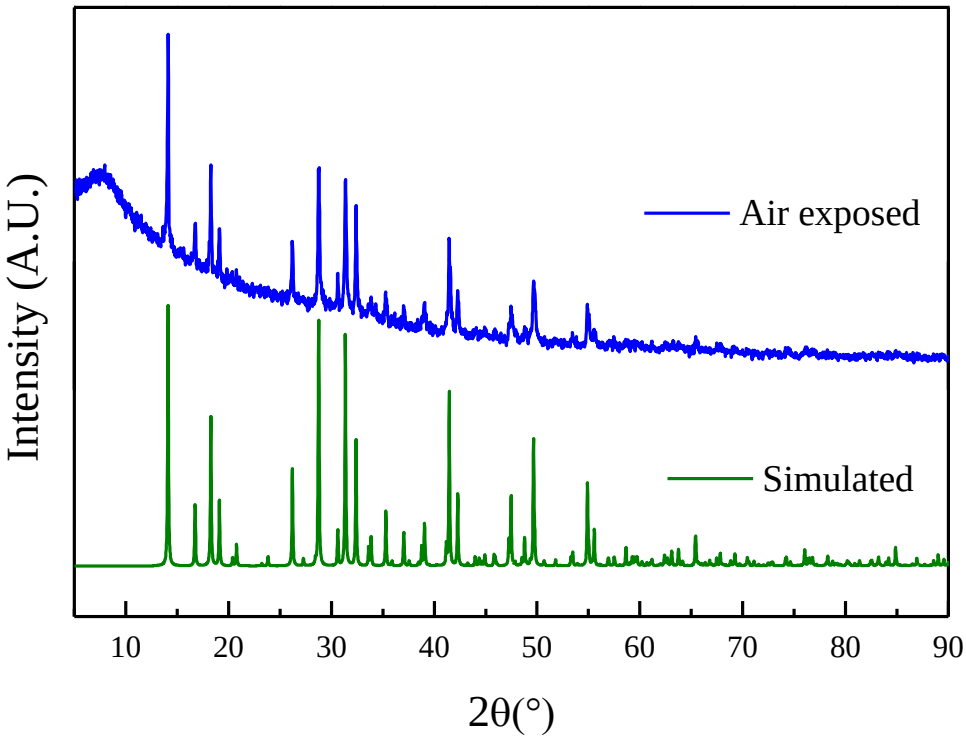

Figure S4: PXRD patterns showing the comparison of air exposed $LiMnPS_4$ with the simulated pattern of $LiMnPS_4$.

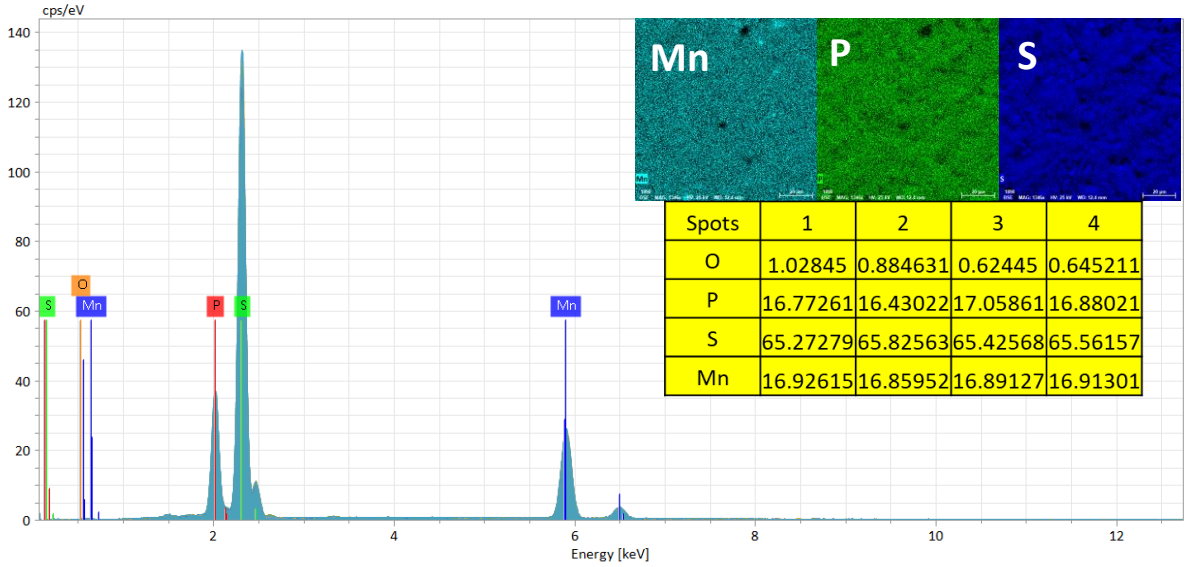

Spots	1	2	3	4
O	1.02845	0.884631	0.62445	0.645211
P	16.77261	16.43022	17.05861	16.88021
S	65.27279	65.82563	65.42568	65.56157
Mn	16.92615	16.85952	16.89127	16.91301

Figure S5: EDS analysis of the as synthesized $LiMnPS_4$. The table indicates the atomic percentage of the elements at different spots. A small percentage of oxygen is not avoidable as sulfides are known to undergo some surface oxidation.

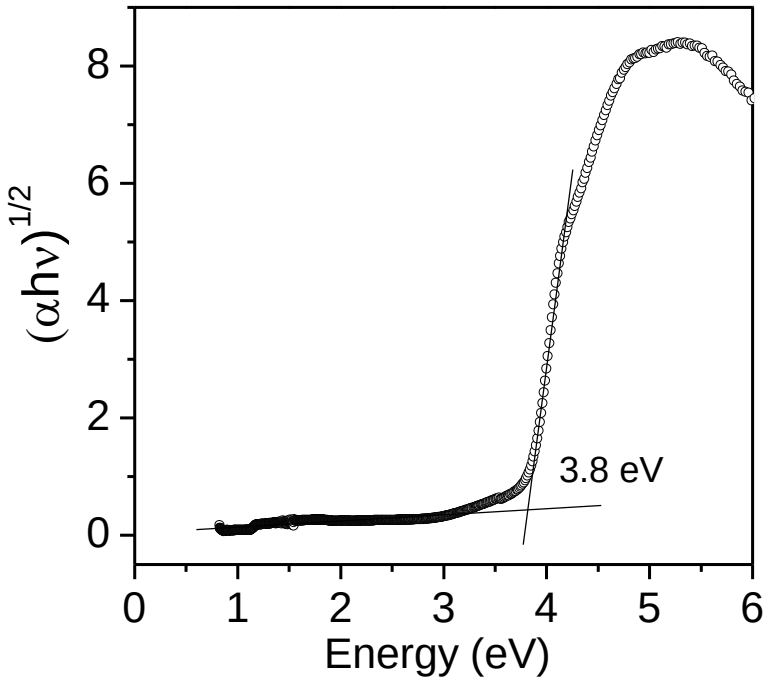

Figure S6: Diffuse reflectance plot for γ-Li_3PS_4.

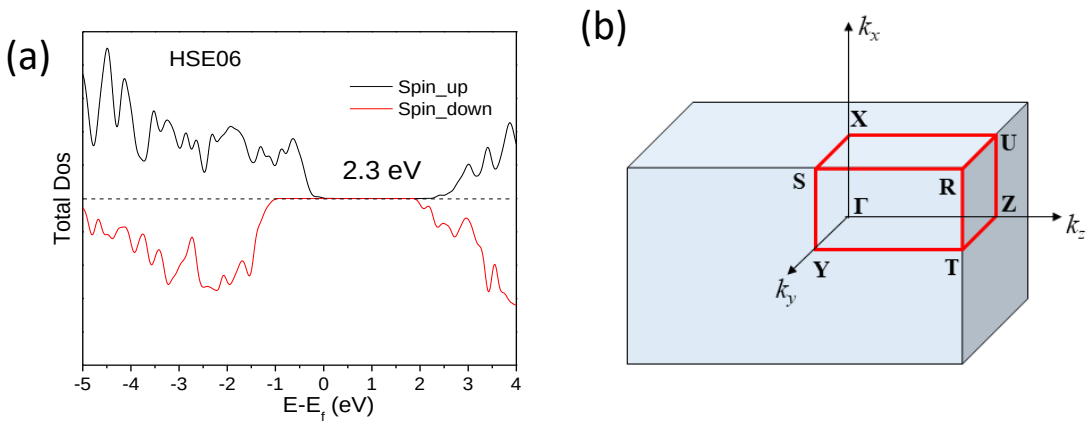

Figure S7: (a) Total density of states calculated using HSE06 hybrid functionals; (b) Brillouin zone of primitive orthorhombic lattice with high symmetry points.

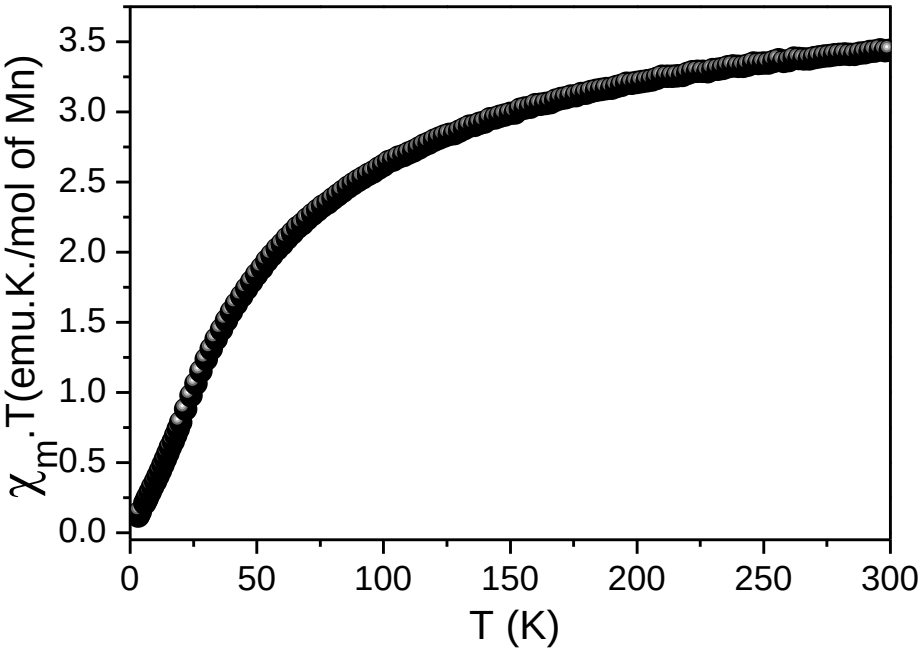

Figure S8: χ_mT versus T plot indicating the antiferromagnetic behavior of $LiMnPS_4$ phase at low temperatures.

References:

1. Bruker- SMART, Bruker AXS Inc., Madison, Wisconsin, USA, 2002.
2. Bruker-SAINT and SADABS, and SHELXTL, Bruker AXS Inc., Madison, Wisconsin, USA, 2008.
3. G. M. Sheldrick *Acta Crystallogr., Sect. A: Found. Crystallogr.*, 2008, **64** , 112 – 122
4. C. B. Hübschle , G. M. Sheldrick and B. Dittrich , *J. Appl. Crystallogr.*, 2011, **44** , 1281 – 1284.
5. P. Kubelka and F. Z. Munk , *Tech. Phys.*, 1931, **12** , 593 – 601.
6. G. Kresse and J. Hafner , *Phys. Rev. B: Condens. Matter Mater. Phys.*, 1993, **47** , 558 – 561.
7. G. Kresse and J. Furthmüller , *Comput. Mater. Sci.*, 1996, **6** , 15 – 50.
8. G. Kresse and J. Furthmüller , *Phys. Rev. B: Condens. Matter Mater. Phys.*, 1996, **54** , 11169 – 11186.
9. D. Joubert *Phys. Rev. B: Condens. Matter Mater. Phys.*, 1999, **59** , 1758 – 1775.
10. A. V. Krukau, O. A. Vydrov, A. F. Izmaylov and G. E. Scuseria, *J. Chem. Phys.*, 2006, **125**, 224106.